COMPLEX DYNAMICS OF THE BUBBLE RISING IN THE VERTICAL HELE–SHAW CELL WITH A MAGNETIC FLUID

A. Tatulchenkov, A. Cēbers
Institute of Physics, University of Latvia, Salaspils-1, LV-2169, Latvia

Introduction. The free interface dynamics in a Hele–Shaw cell obtained a big interest recently from the point of view of the pattern formation phenomena. Extraordinary rich phenomena occur in the Hele–Shaw cells with a magnetic fluid [1, 2, 3]. The drops of magnetic fluid and bubbles in the Hele–Shaw cells filled with it have the spectrum of instabilities leading to the formation of the labyrinthine patterns [4, 5].

An interesting example of the complex dynamics of the free interface rises when the bubble motion in the vertical Hele–Shaw cell with the magnetic fluid is considered [6]. The problem of the bubble motion in the Hele–Shaw cell has a rather long history. It was for the first time considered by Saffman and Taylor in [7]. Preliminary qualitative numerical experiments illustrated that at magnetic Bond numbers larger than the critical ones for the elliptic instability [6] two stationary families of steady shapes of the bubble, rising in the vertical Hele–Shaw cell with a magnetic fluid, exist – a pear-like famillt when the initial perturbation is along the direction of the gravity force, and a bent dumb-bell one if the initial perturbation of the bubble shape is perpendicular to it.

Investigation of the behavior of the steady families of the bubble shapes have revealed several interesting peculiarities of their behavior – at some critical value of the magnetic Bond number bifurcation phenomenon to the unsteady shape is observed and the oscillatory bubble behavior is found.

1. Governing equations. The motion of the magnetic fluid surrounding the bubble is described by the Darcy equation, where the action of gravitational and magnetic forces is taken into account [6]

$$-\nabla p - \alpha \mathbf{v} + \frac{2M}{h}\nabla\varphi_{\mathrm{m}} + \rho\mathbf{g} = 0\,; \quad \mathrm{div}\mathbf{v} = 0\,. \tag{1}$$

Here $\alpha = 12\eta/h^2$ is the friction coefficient of the fluid in the Hele–Shaw cell of thickness h, φ_{m} is the value of the magnetostatic field potential created by the magnetic fluid on the boundary of the Hele–Shaw cell $z = h$. The pressure on the interface of the bubble is given by the Laplace law

$$p_0 = p + \sigma k\,. \tag{2}$$

The magnetostatic field potential created by the magnetic fluid outside the bubble φ_{m} can be expressed through the magnetostatic potential of the droplet with the shape of bubble φ_{md}:$\varphi_{\mathrm{m}} = -2\pi Mh - \varphi_{\mathrm{md}}$, here φ_{md} is

$$\varphi_{\mathrm{md}} = -M\iint\left(\frac{1}{\sqrt{|\rho-\rho'|^2}} - \frac{1}{\sqrt{|\rho-\rho'|^2+h^2}}\right)\mathrm{d}S'\,, \tag{3}$$

where integration is carried out in the region, which has the shape of a bubble. The free interface dynamics is found from the kinematic boundary condition

$$\frac{\mathrm{d}\mathbf{r}}{\mathrm{d}t} = \mathbf{v}\big|_{\Sigma}\,. \tag{4}$$

Here k is the curvature of the interface in the plane of the boundary of the Hele–Shaw cell, $\mathbf{v}\big|_\Sigma$ is the velocity of the fluid on the interface of the bubble. Pressure p_0 inside the bubble is taken to be constant since the friction there is neglected. To put problems (1), (4) in the dimensionless form, the following scales are introduced: length – R – the radius of an unperturbed circular bubble, time – $\alpha R^3/\sigma$ – a characteristic capillary relaxation time of the bubble in the Hele–Shaw cell. Equation (1) in the dimensionless form reads (gravity acceleration is directed in the negative x-axis direction):

$$-\nabla p - \mathbf{v} + \frac{\mathrm{Bm}}{\widetilde{h}^2}\nabla\varphi_\mathrm{m} - \mathrm{Bg}\mathbf{e}_x = 0\,; \quad \mathrm{div}\mathbf{v} = 0\,, \tag{5}$$

where the magnetic Bond number $\mathrm{Bm} = 2M^2h/\sigma$, the gravitational Bond number $\mathrm{Bg} = \rho g R^2/\sigma$ and the dimensionless thickness of the Hele–Shaw cell $\widetilde{h} = h/R$ are introduced. Tildes further are omitted.

2. Numerical simulation. Problems (1)–(4) possess the invariance property allowing for arbitrary choice of the tangential component of the velocity on the free interface [8]. Here it will be chosen to sustain the equal arc length between neighboring markers of the interface at its evolution in time. We are using a contour dynamics approach for the motion of the free interface of the bubble. According to it, the equations for the tangent angle ϑ $\big(\tau = (\cos\vartheta, \sin\vartheta)\big)$ and the arclength of the contour are

$$\vartheta_t = -\frac{1}{s_p}U_p + \frac{T}{s_p}\theta_p\,, \tag{6}$$

$$s_{tp} = T_p + \theta_p U\,, \tag{7}$$

where the velocity on the interface $\mathbf{v}\big|_\Sigma$ is given by $U\mathbf{n}+T\tau$. To maintain the equal arclength pacing between the markers contour arclength is given by $s = L/2\pi p$. Then equation (7) gives

$$T(p,t) = T(0,t) + \frac{p}{2\pi}\int\limits_0^{2\pi}\theta_{p'}U\,\mathrm{d}p' - \int\limits_0^{p}\theta_{p'}U\,\mathrm{d}p'\,, \tag{8}$$

where the constant of integration $T(0,t)$ is put equal to zero. The time evolution of the interface is given by (6), (8). Since ϑ is not a periodic function of p its linearly increasing part is excluded according to the relation $\theta = p + \vartheta$. As a result,

$$L_t = \int\limits_0^{2\pi}(\vartheta_p + 1)U\,\mathrm{d}p \tag{9}$$

$$\vartheta_t = \frac{2\pi}{L}\Big[-U_p + T(\vartheta_p + 1)\Big]. \tag{10}$$

The second key idea of the numerical approach is a small-scale decomposition of evolution equation (10), since the numerical stiffness arises due to small spatial scales [8]. Differential equations (**??**) are solved using the fourth-order Adams–Bashforth method [9].

3. Results of numerical simulation. The shapes established at long time evolution in dependence on the magnetic Bond number are given in Fig. 1, where the contour length of the interface in dependence on Bm is shown (in the case of the oscillatory regime the maximal value of the contour length during the

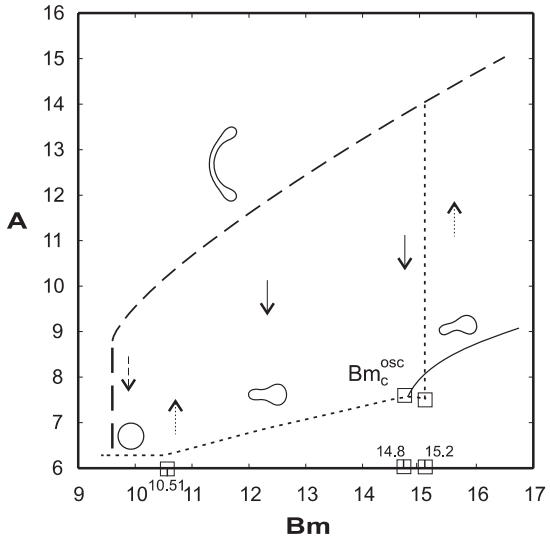

Fig. 1. The phase diagram of the bubble shapes Bg = 1, $h = 1$).

period is shown). We see that above the critical value of the elliptical instability the bubble with the initial perturbation in the form of the second eigenmode undergoes transition to the steady state having a pear-like shape. This shape exists until the critical value Bm_c^{osc}, which at the given value of $h = 1$ is about 14.8, when the transition to the unsteady state occurs. The branch of the pear-like shapes exists until the critical magnetic Bond number 15.2 when an abrupt transition to the bent dumb-bell shape occurs with a subsequent transition to the oscillatory regime.

The bent dumb-bell branch of steady shape of the bubble exists in the range of magnetic Bond numbers even below the critical value of the elliptical instability as shown in Fig. 1. This hysteresis illustrates that the transition to the bent dumb-bell shapes is the transition of the first kind. The bent dumb-bell shape with the increased contour length exists for the values of magnetic Bond numbers Bm above the critical ones. If this shape is perturbed, for example, by applying the gravity force in the y-axis direction, it relaxes to a steady or an oscillating pear-like shape. The dynamics of the bubble in oscillatory state for Bm = 16 ($h = 1$) is shown in Fig. 2.

Although the oscillatory behavior of the bubble looks rather unusual we should mention that such behavior was already noticed in several systems under the action of external fields. In [10] the oscillatory behavior of the islands on the surface induced by the electromigration is predicted basing on the local interface evolution model. The oscillatory character of the self-magnetic energy release by long

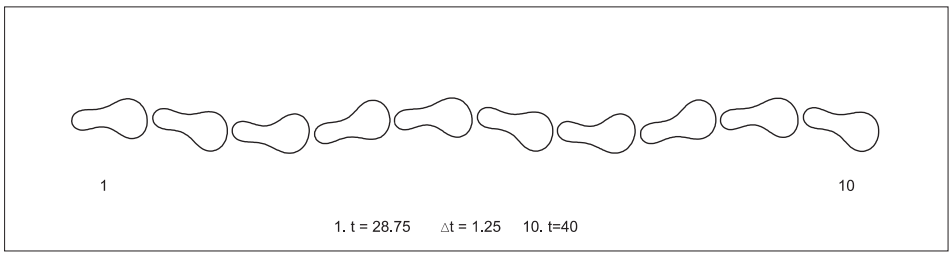

Fig. 2. Oscillatory dynamics of the bubble with a pear-like shape. Bg = 1, $h = 1$).

wavelength perturbations at the magnetic microconvection is found in [11]. These facts and our numerical simulation results show that the dynamics at the external energy supply under the action of magnetic forces can be rather complicated. This is the case for the system considered here when the regimes of the bubble motion become rather complicated at the increase of the magnetic Bond number.

4. Discussion and conclusions. The dynamics of the rising bubble in the vertical Hele–Shaw cell with the magnetic fluid is studied. Considering the phase diagram of the bubble shapes it is found that two families of the steady states of the bubbles at magnetic Bond numbers below the critical values exist – pear-like shapes and bent dumb-bell shapes. For the latter a numerical evidence supports its establishment by a subcritical bifurcation from the circular one. By the finite amplitude perturbation it is possible to initiate the transition of a bent dumb-bell shape to a pear-like one. As far as we know, it is for the first time when the spiraling motion of the bubble in the low Reynolds number limit is found although there are observations of the possibility of complex dynamics in different systems under the action of external fields. This illustrates that the dissipation processes in the presence of the self-magnetic field forces can be rather unusual and complicated. We should mention that some qualitative experimental observations resembling the results of our numerical calculations have already appeared [12]. This confirms the necessity of further experimental investigations of the dynamics of the bubble in the Hele–Shaw cell with a magnetic fluid.

5. Acknowledgments. This work has been carried out due to the financial support of the Fifth Framework Programme Growth Project G1MA-CT-2002-04046.

REFERENCES

1. A. Cebers, M.M. Mayorov. Magnetostatic instabilities in plane layers of magnetizable fluids. *Magnetohydrodynamics*, vol. 16 (1980), no. 1, pp. 21–27.
2. S.A. Langer, R.E. Goldstein, D.P. Jackson. Dynamics of labyrinthine pattern formation in magnetic fluids. *Phys. Rev. A*, vol. 46 (1992), pp. 4894.
3. F. Elias, C. Flament, J.–C. Bacri, S. Neveu. Macro-organized patterns in ferrofluid layer: experimental studies. *J. Phys. I*, vol. 7 (1997), pp. 711.
4. A. Cebers, M. Mayorov. Structures of interface a bubble and magnetic fluid in a field. *Magnetohydrodynamics*, vol. 16 (1980), no. 3, pp. 231–235.
5. R.E. Rosensweig, M. Zahn, R. Shumovich. Labyrinthine instability in magnetic and dielectric fluids. *J.Magn. Magn. Mater.*, vol. 39 (1993), pp. 127.
6. A. Cebers. Numerical experiments on the modelling of the rising of bubbles to the surface in a vertical flat layer of magnetic fluid. *Magnetohydrodynamics*, vol. 21 (1985), no. 4, pp. 381–386.
7. G. Taylor, P.G. Saffman. A note on the motion of bubbles in a Hele–Shaw cell and porous medium. *Quart. Journ. Mech.and Applied Math.*, vol. 12 (1959), pp. 265.
8. T.Y. Hou, J.S. Lowengrub, M.S. Shelley. Removing the stiffness from interfacial flows with surface tension. In *J. Comp. Phys.*, vol. 114 (1994), pp. 312.
9. A. Samarskij, A. Gulin. it Numerical methods (Science, Moscow, 1989).
10. P. Kuhn, J. Krug, F. Hausser, A. Voigt. Complex shape evolution of electromigration-driven single-layer islands. *arXiv:cond-mat* (0410745).
11. M. Igonin, A. Cebers. Labyrinthine instability of miscible magnetic fluids. *Phys. Fluids*, vol. 15 (2003), pp. 1734.
12. V. Bahtovoi, M. Kovalev, A. Reks. Instabilities of bubbles and droplets flows in magnetic fluids. In *Proceedings of 10th International Conference on Magnetic fluids* (Brazil, 2004).